applied sciences

MDPI

*Article*

# Zinc Adsorption by Activated Carbon Prepared from Lignocellulosic Waste Biomass

**Sari Tuomikoski [1,*], Riikka Kupila [2], Henrik Romar [1,2], Davide Bergna [2], Teija Kangas [1], Hanna Runtti [1] and Ulla Lassi [1,2]**

[1] Research Unit of Sustainable Chemistry, University of Oulu, P.O. Box 4300, FI-90014 Oulu, Finland; sari.tuomikoski@oulu.fi (S.T); henrik.romar@chydenius.fi (H.R.); teija.kangas@oulu.fi (T.K.); hanna.runtti@oulu.fi (H.R.); ulla.lassi@oulu.fi (U.L.)

[2] Unit of Applied Chemistry, Kokkola University Consortium Chydenius, University of Jyvaskylä, Talonpojankatu 2B, FI-67100 Kokkola, Finland; riikka.kupila@chydenius.fi (R.K.); davide.bergna@chydenius.fi (D.B.)

* Correspondence: sari.tuomikoski@oulu.fi; Tel.: +358-294-481644

Received: 2 October 2019; Accepted: 22 October 2019; Published: 28 October 2019

**Featured Application:** In this study, activated carbon from lignocellulosic waste biomass was prepared and it was used to the zinc removal. The adsorption capacity obtained for the prepared material was compared favorably to other adsorbents used in zinc removal presented in literature. Therefore, the suitable adsorbent for zinc removal from waste biomass was developed by using non-hazardous materials. The adsorbent can be used with wide temperature range and with quite high concentration range.

**Abstract:** Sawdust was used as a precursor for the production of biomass-based activated carbon. Carbonization and activation are single-stage processes, and steam was used as a physical activation agent at 800 °C. The adsorption capacity towards zinc was tested, and the produced activated carbon proved effective and selectively adsorbent. The effects of pH, initial concentration, adsorbent dosage, time, temperature, and regeneration cycles were tested. The adsorption capacity obtained in this study was compared favorably to that of the materials reported in the literature. Several isotherms were applied to describe the experimental results, with the Sips isotherm having the best fit. Kinetic studies showed that the adsorption follows the Elovich kinetic model.

**Keywords:** lignocellulosic biomass; adsorption; carbonization; adsorbent; zinc; regeneration

## 1. Introduction

Water purification and the removal of toxic substances from wastewaters are increasing global challenges. Both surface and ground waters worldwide are reported to be contaminated with impurities deriving from natural and human-involved sources [1]. Metals such as cadmium, chromium, copper, nickel, and zinc (Zn) are commonly associated with pollution problems [2]. Significant anthropogenic sources of Zn in the environment include: metallifereous mining [2]; agricultural sources, such as fertilizers and manure; sewage sludge [3]; metallurgical industries, such as the production of special alloys and steel [4]; landfill leachates [5]; electroplating in the metal finishing industry [6]; and miscellaneous sources, such as batteries [7]. For humans, Zn is an important micronutrient, but too-high amounts of Zn can cause depression, lethargy, and neurologic issues such as seizures and ataxia [8–11]. Therefore, the effective removal of Zn from water is vital.

Various methods and combinations of methods exist for the removal of Zn, including electrocoagulation [7], ion exchange [5], membrane filtration [6], coagulation–flocculation, flotation,

and chemical precipitation [8]. The most frequently used methods are ion exchange and membrane filtration [8]. In addition, adsorption is a suitable method for removing heavy metals such as Zn because it is simple, highly efficient, and cost-effective and has regeneration potential [11,12]. Activated carbon is the most widely applied adsorbent for water purification and is traditionally prepared using, for example, coconut shells or coal as a precursor [13]. The literature contains several studies about the preparation of activated carbon from different agro-based biomass raw materials, such as cherry stones, eucalyptus bark saw dust, bagasse, and peanut husks [14–18].

The preparation of activated carbon basically consists of two stages, carbonization and activation. Carbonization and activation can be performed in one single reaction or in a two-stage reaction where carbonization and activation are separated in time and space [19]. The carbonization yield (degree of conversion) varies widely as a function of the amount of carbon being removed as $CO_x$ or hydrocarbons. The production of activated carbon is typically dominated by a compromise between porosity development and process yield [20]. The typical yield for lignocellulosic materials in the carbonization step is 20 wt%–30 wt% and after the activation step the overall yield is approximately 10 wt% [21]. The pore structure of the carbon after the carbonization step is insufficient, and therefore the activation step is needed. In the activation process, spaces between aromatic sheets are cleared of various carbonaceous compounds and disorganized carbon that might have filled the interstices during carbonization. Carbonized material is converted into a form that contains a large number of randomly distributed pores of various shapes and sizes, giving rise to a product with an extended and extremely high surface area. The carbonized material is further treated using chemical or physical activation to increase the surface area and the porosity [22,23].

Physical activation is a two-stage process in which the carbonization step is followed by physical activation. Physical activation is typically done between 600 °C and 900 °C, the temperature range in which the selective gasification of individual carbon atoms take place. Steam and carbon dioxide are the most commonly used physical activation agents [22]. The loss of sample mass during the activation step occurs due to the combined effect of devolatilization and the loss of fixed carbon that remains after the release of volatiles [20,21]. The porosity is generated in the slow oxidation process where carbon atoms react with oxygen generating carbon dioxide [21].

The aim of this work is to develop eco-innovative biomass-derived water treatment material from a renewable source and to study the conditions in which the material can be used effectively. Due to the bioeconomy and circular economy potential, renewable sources, waste materials, and locally available materials are the future in the production of activated carbon. There is huge potential in terms of the use of raw materials, such as saw dust from sawmills and other locally available waste biomass materials. To that end, sawdust waste from sawmills was used as a precursor in the production of activated carbon. The carbonization and activation conditions of this lignocellulosic biomass were optimized, and the material produced was characterized and tested in terms of Zn adsorption based on wide range of pH levels, initial Zn concentration, adsorbent mass, temperature, and time ranges. Reuse of the material was also studied by testing the material regeneration using 0.1 M hydrogen chloride (HCl). Several isotherm models were used, such as Langmuir, Freundlich, and Sips adsorption isotherms. Pseudo-first-order, pseudo-second-order, and Elovich kinetic models were also used.

## 2. Materials and Methods

### *2.1. Preparation of Activated Carbons*

A dried and sieved lignocellulosic biomass composed of birch sawdust from a Swedish saw-mill was carbonized and steam activated in a one-step process in a rotating quartz reactor (Nabertherm GmbH RSRB 80-750/11, Lilienthal, Germany). The single-stage thermal process was divided into two sub-stages, a carbonization step in which the temperature was raised to 800 °C and an activation stage. During the activation, the temperature was set to hold at 800 °C for 120 min with a stream of steam to ensure proper surface activation. During the whole process, the reactor was flushed with

inert $N_2$ gas. The carbons were crushed and sieved, and a 100–425 μm fraction was characterized and used for the Zn adsorption tests.

### *2.2. Characterization Methods*

The pore size, pore volume, and specific surface area of the produced activated carbons were analyzed based on nitrogen adsorption–desorption isotherms at the temperature of liquid nitrogen using a Micromeritics ASAP 2020 system (Norcross, GA, USA). Prior to measurements, samples were pretreated at low pressures and high temperatures to clean the surfaces. Sample tubes were immersed in liquid nitrogen (−197 °C), nitrogen gas was added to the samples in small steps, and the resulting isotherms were obtained. Specific surface areas were calculated from adsorption isotherms according to the Brunauer–Emmett–Teller (BET) method [24] and pore size distributions were calculated using the Barrett–Joyner–Halenda (BJH) algorithm [25]. Sample degassing was performed by elevating the temperature to 50 °C under restricted pressure drop to 15 mm Hg followed by a 10-min hold at 50 °C. After the hold period, the samples were heated 10 °C/min up to 140 °C under free evacuation. Finally, samples were degassed at 140 °C for 3 h. This procedure gives a final, constant pressure of 2 μm Hg.

The content of carbon present in each sample, given as total carbon (TC) percent, was measured using a solid-phase carbon analyzer (Skalar Primacs MCS, Breda, The Netherlands). Dried samples were weighted in quartz crucibles and combusted at 1100 °C in an atmosphere of pure oxygen, and the formed $CO_2$ was analyzed by the infrared (IR) detector of the instrument. Carbon content values were obtained by reading the signal of the IR analyzer from a calibration curve derived from known masses of a standard substance, oxalic acid. The total mass of carbon was calculated as a percent of the mass initially weighted and was measured after the carbonization and activation steps.

### *2.3. Adsorption and Desorption Experiments*

The effect of pH on the Zn adsorption properties of the activated carbons was tested using 25 mL sample volume, 100 mg/L Zn solution prepared from $ZnCl_2$, adsorbent dosage 5 g/L, and pH range 2–7. Experiments were done in an Erlenmeyer flask, and the mixture was agitated continuously for 24 h to achieve equilibrium between the adsorption and regeneration of Zn. After the pH optimization experiments were done, the effect of the initial Zn concentration was studied at the optimum pH with initial Zn concentration range 10 mg/L–500 mg/L by using 24 h adsorption time. After that, adsorbent dosage optimization tests were done with an adsorbent mass of 0.5–10 g/L at under the previously determined optimum conditions. After these parameters were optimized, the effect of time was studied, with time ranging from 1 min to 24 h. The effect of temperature was studied using temperatures of 10 °C, room temperature, 22 °C, and 40 °C. All the adsorption experiments have been done duplicated. Regeneration experiments were done with a 2.5 g/L dosage of activated carbon adsorbed with Zn in optimized conditions and mixed in 0.1 M HCl. Samples were taken within time range 1 min and 4 h.

Because the pH of the activated carbon prepared from the lignocellulosic biomass is quite alkaline (pH of approximately 10), the pH of the solution was adjusted in all experiments with 0.1 M or 0.01 M HCl to ensure the correct pH value and to prevent the formation of unwanted precipitation. pH adjustments were done after mixing the adsorbent and the Zn solution. Before taking the Zn concentration measurements, the sample was filtered and diluted. The concentration of the Zn in the solution was measured using atomic absorption spectroscopy (AAnalyst 200 atomic absorption spectrometer; Perkin–Elmer, Waltham, Massachusetts, USA).

### *2.4. Isotherm Analysis*

Below, the results of three non-linear adsorption models are reported. The non-linear form of Langmuir's Equation [26] is:

$$q_e = \frac{b_L q_m C_e}{1 + b_L C_e}, \quad (1)$$

where $b_L$ (L/mg) represents the energy of sorption, $q_m$ (mg/g) is the Langmuir constant that is related to the sorption capacity, and $C_e$ (mg/L) is the Zn concentration of the solution in equilibrium. The Freundlich model [27] can be written as:

$$q_e = K_F C_e^{1/n_F}, \quad (2)$$

where $K_f$ (L/g) and $n_F$ are Freundlich constants related to the sorption capacity and intensity, respectively. The Sips isotherm [28] combines properties of both the above mentioned models and is given as:

$$q_e = \frac{q_m (b_S C_e)^{n_S}}{1 + (b_S C_e)^{n_S}}. \quad (3)$$

In this equation constant $b_S$ (L/mg) is a constant related to sorption energy, the $q_m$ (mg/g) value relates to the sorption capacity, and $C_e$ (mg/L) is the Zn concentration of the solution in equilibrium. Isotherm parameters were obtained using non-linear regression with OriginPro 2018.

### *2.5. Kinetic Studies*

Three non-linear models, the pseudo first-order [29], pseudo second-order [30], and Elovich models [31], were used to describe the kinetic behavior of the sorption process.

The equation of the pseudo first-order model can be written as:

$$q_t = q_e(1 - e^{-k_1 \cdot t}) \quad (4)$$

where $k_1$ ($min^{-1}$) is the pseudo-first-order rate constant, $q_t$ (mg/g) is the amount of Zn ions adsorbed at time $t$ (min), and $q_e$ (mg/g) is the amount of Zn ions adsorbed at equilibrium [29].

The pseudo-second-order equation is:

$$q_t = \frac{{q_e}^2 k_2 t}{q_e k_2 t + 1}. \quad (5)$$

where the parameter $k_2$ is the pseudo-second-order rate equilibrium constant (g/mg min) [30].

The non-linear form of the Elovich equation is:

$$\mathrm{q} = \frac{1}{\beta} \ln\left(\upsilon_0 \beta + \frac{1}{\beta} lnt\right), \quad (6)$$

where $\beta$ (g/mg) is the desorption constant and $\upsilon_0$ (mg/g min) is the initial sorption rate [31]. Kinetic parameters were obtained using non-linear regression with OriginPro 2018.

For both the kinetic and isotherm models, the residual root mean square error (RMSE) was determined to evaluate the fit of the isotherm equations to the experimental data. The smaller the error function value, the better the curve fit. The calculated expressions of error function can be defined as follows:

$$\mathrm{RMSE} = \sqrt{\frac{1}{n-p} \sum_{i=1}^{n} (q_{e(exp)} - q_{e(calc)})^2}, \quad (7)$$

where $n$ is the number of experimental data points, $p$ is the number of parameters in the isotherm model, and $q_{e(exp)}$ (mg/g) and $q_{e(calc)}$ (mg/g) are the experimental and calculated values of sorption capacity in equilibrium, respectively.

### *2.6. Weber–Morris Model*

The diffusion mechanism was analyzed using the intraparticle diffusion model introduced by Weber and Morris, as follows:

$$q_t = k_{id} t^{1/2} + C, \quad (8)$$

where $k_{id}$ (mg $g^{-1}$ $min^{-1/2}$) is the intraparticle diffusion in the rate-determining step, and C is the intercept related to the thickness of the boundary layer [32].

### *2.7. Thermodynamics*

The thermodynamic parameters calculated from the experimental result reveals the spontaneity of the process. To solve these parameters, the Van't Hoff equation was applied. The equation is expressed as follows:

$$\ln K_d = -\frac{\Delta H^0}{RT} + \frac{\Delta S^0}{R}, \quad (9)$$

where $R$ is the universal gas constant (8.314 J/mol K), $T$ (K) is the temperature used in the experiments, and $K_d$ (L/g) is the equilibrium constant calculated from the experimental results in equilibrium conditions using the following equation:

$$K_d = \frac{q_e}{C_e} \quad (10)$$

In addition, $\Delta H^0$ where calculated by Van't Hoff equations:

$$\Delta G^0 = -RTlnK_d \quad (11)$$

## 3. Results and Discussion

Biomass-based activated carbon was used in the removal of Zn. The effects of pH, competitive ions, initial concentration, adsorbent dosage, temperature, time, and desorption were studied. Isotherm analysis, kinetic modeling, and thermodynamic calculations were done. Experiments were also done for commercial activated carbon as a reference sample, but the results are not presented because the removal percentage was 10–30% depending on the initial Zn concentration and the adsorbent dosage (1 g/L–10 g/L).

### *3.1. Characterization of Activated Carbon*

Table 1 presents the yield of the carbonization and activation steps, TC content, surface area, pore volume, and mean pore sizes of the prepared activated carbon. Based on the literature, the carbon content for biomass-based activated carbons typically varies between 65% and 97%. Therefore, the TC content obtained in this study is very high [33], specific surface area can vary between 336 $m^2/g$ and 1080 $m^2/g$ for biomass-based activated carbon, and the pore volume can vary between 0.02 $cm^3/g$ and 0.80 $cm^3/g$ [33]. Therefore, the results obtained in this study are in the same order of magnitude [33]. The total yield of the carbonization and activation steps is 10%, which is typical for a lignocellulosic biomass [21].

**Table 1.** Characterization results of produced activated carbon sample.

| | | | Brunauer–Emmett–Teller (BET) | | | Barrett–Joyner–Halenda (BJH) | | |
|---|---|---|---|---|---|---|---|---|
| **Sample** | **Yield [%]** | **TC [%]** | **Specific Surface Area [$m^2/g$]** | **Pore Volume [$cm^3/g$]** | **Average Pore Size [nm]** | **Micropore [%]** | **Mesopore [%]** | **Macropore [%]** |
| Birch carbon | 10 | 97 | 860 | 0.61 | 2.8 | 14 | 84 | 2 |

### *3.2. Effect of pH and Competitive Ion*

pH optimization tests were done with the pH ranging between 2 and 7; the results are presented in Figure 1. The results clearly show that the optimum pH value for adsorption is 4 and that removal efficiency is slightly lower with pH values of 6 and 7. There is no removal capacity with a pH value of 2.

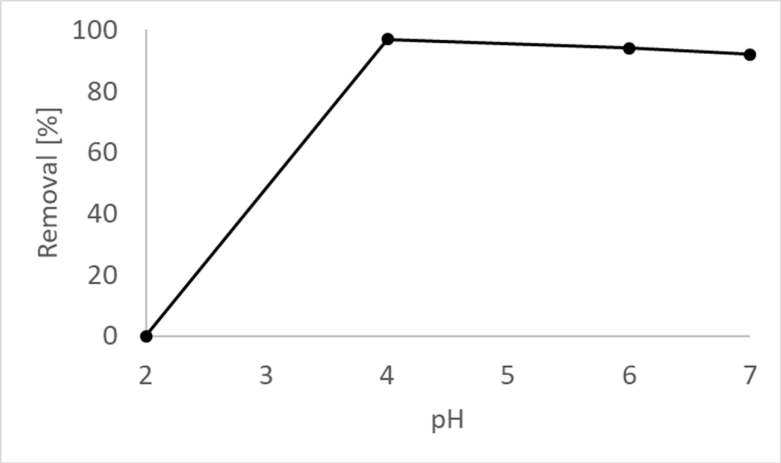


**Figure 1.** The removal percentage as a function of pH. Experiments were done in duplicate and the range of results were at maximum 3 percentage points.

The effect of competitive ions was studied using a Zn solution prepared from $ZnCl_2$ or $ZnSO_4$ within a pH range of 2–6. The results clearly show that the adsorbed amount of Zn and the removal percentage seem to be dependent only on pH value and not on the competitive ions ($Cl^-$ or $SO_4^{2-}$). Thus, adsorption towards the biomass-based activated carbon is selective.

### *3.3. Effect of Initial Concentration*

The effect of the initial Zn concentration was studied at the optimum pH value of 4. Other concentrations were also studied: 10 mg/L, 25 mg/L, 50 mg/L, 75 mg/L, 100 mg/L, 125 mg/L, 150 mg/L, 200 mg/L, and 500 mg/L. The results of the initial concentration experiments are presented in Figure 2. Biomass-based activated carbon works quite well in the concentration range of 0 mg/L–150 mg/L. The removal percentage increases as a function of the initial Zn concentration to 75 mg/L and then starts to decrease sharply. Therefore, the optimum Zn concentration, 75 mg/L, was selected for further experiments. The optimal adsorption sites are occupied first at low concentrations. When the concentration increases, there may exist some driving forces to increase the removal percentage. [34].

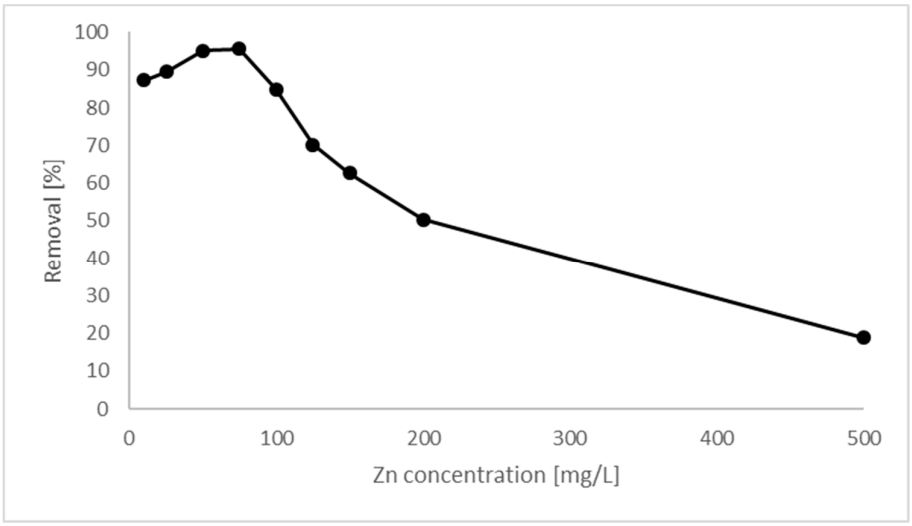


**Figure 2.** Removal percentages as a function of Zn initial concentration. Experiments were done duplicated and the removal % varied in the range of 3 percentage points.

Adsorption capacity increases as a function of Zn concentration. The adsorption capacity was compared to other adsorbents used in Zn removal, shown in Table 2. The adsorption capacities

presented in the literature vary between 2.21 and 52.09 mg/g. The adsorption capacity (21.44 mg/g) obtained in this study was in the same order of magnitude. The amount of Zn adsorbed as a function of Zn concentration is presented in Figure 3. Katsou et al. used the initial metal concentration of 320 mg/L [35] and Mohan and Singh reported the initial metal concentration between 1–1000 mg/L [18]. The initial metal concentration used in this study was 10–500 mg/L. The initial metal concentration may have effect to the adsorption capacity.

**Table 2.** Adsorption capacities of zinc (Zn) on various adsorbents.

| Adsorbent | Adsorption Capacity [mg/g] | Reference |
|---|---|---|
| Natural zeolite | 2.21 | [36] |
| Vermiculite | 3.88 | [37] |
| Defatted rice brans | 5–17 | [38] |
| Solid residue of olive mill products | 5.40 | [39] |
| Activated carbon from almond shells | 6.65 | [40] |
| Natural zeolite | 13.02 | [35] |
| Apricot stones carbon | 13.21 | [41] |
| Biomass-based carbon | 21.44 | This study |
| Lignite | 22.83 | [42] |
| Activated carbon derived from bagasse | 31.11 | [18] |
| Peat | 52.09 | [43] |

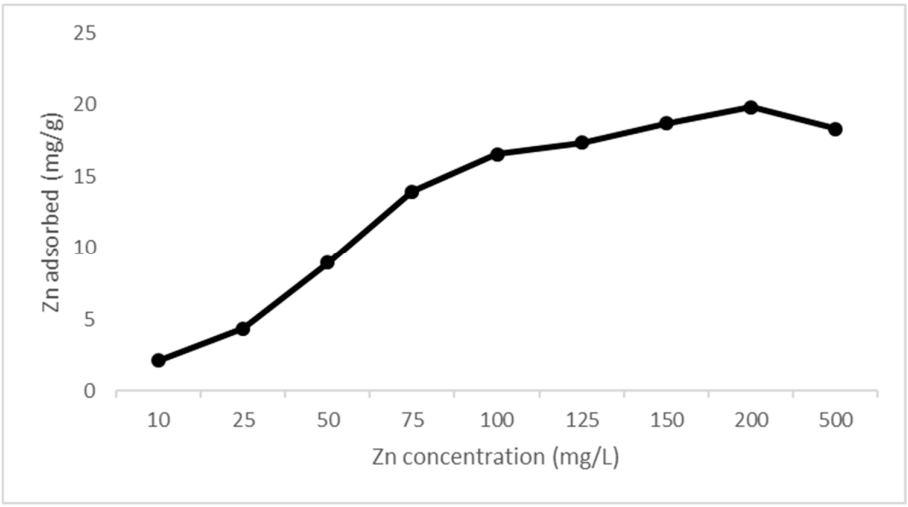


**Figure 3.** Zinc (Zn) adsorption capacity to carbon surface in different initial concentrations. Experiments were done duplicated and the range of results were at maximum 0.3 mg/g.

### *3.4. Effect of Adsorbent Dose*

Figure 4 shows the effect of adsorbent dosage on Zn removal % and adsorption capacity. The highest removal percentage was obtained with doses of 3 g/L and 5 g/L. The adsorption capacities, $q$ [mg/g], increase when the adsorbent dose increases. This is a logical result because the higher amount of adsorbent can uptake more Zn ions from the solution. The higher the dosage, the greater the number of available adsorption sites there are to protect against impurities [18,44].

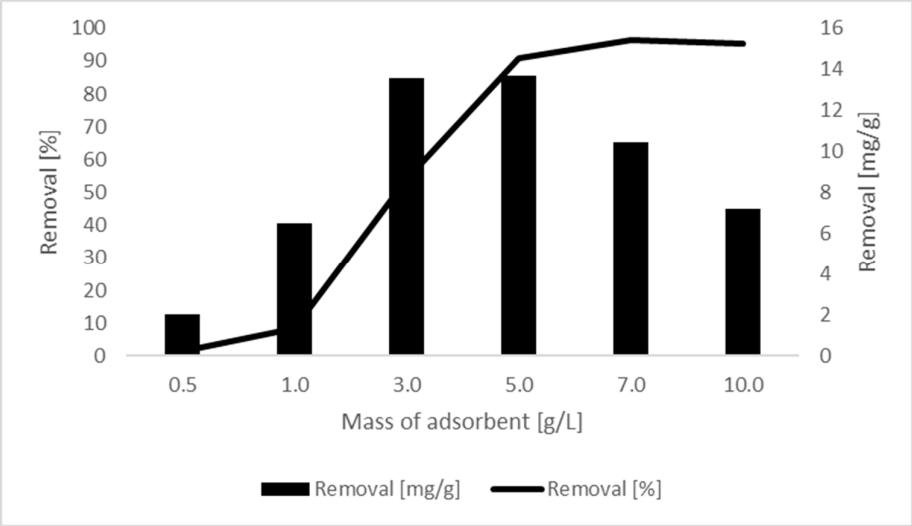


**Figure 4.** Zinc **r**emoval [%] and adsorption capacity [mg/g] as a function of the mass of the adsorbent. Experiments were done duplicated and the range of results were at maximum 3 percentage points in values of removal % and at maximum 0.5 mg/g in adsorption capacity determinations.

### *3.5. Isotherms*

Several non-linear isotherm models (Langmuir, Freundlich, Sips, Bi-Langmuir, Toth, Temkin, and Dubinin–Radushkevich) were applied to the experimental data. However, according to the $R^2$ values and RMSEs, the Sips model was clearly the best fit ($R^2$ = 0.95, RMSE = 1.81). For that reason, only the parameters of the most traditional Langmuir and Freundlich isotherms, in addition to the Sips isotherm, are presented in Table 3. Corresponding fits are illustrated in Figure 5. The applicability of the Sips model is a very reasonable result, as it is generally known to represent adsorption well on heterogenous surfaces, which is the case with biomass-based activated carbon materials.

**Table 3.** Isotherm parameters of Langmuir, Freundlich, and Sips models.

| Parameters and Errors | | Value |
|---|---|---|
| Experiment | Max. $q_e$ [mg/g] | 21.44 |
| **Langmuir** | $q_m$ [mg/g] | 20.78 |
| | $b_L$ [L/mg)] | 0.29 |
| | $R^2$ | 0.87 |
| | RMSE | 2.68 |
| **Freundlich** | $n_F$ | 5.86 |
| | $K_F$ [(mg/g)/(mg/L)$^n$] | 8.50 |
| | $R^2$ | 0.71 |
| | RMSE | 4.06 |
| **Sips** | $q_m$ [mg/g] | 19.10 |
| | $b_S$ [L/mg] | 0.41 |
| | $n_S$ | 4.02 |
| | $R^2$ | 0.95 |
| | RMSE | 1.81 |

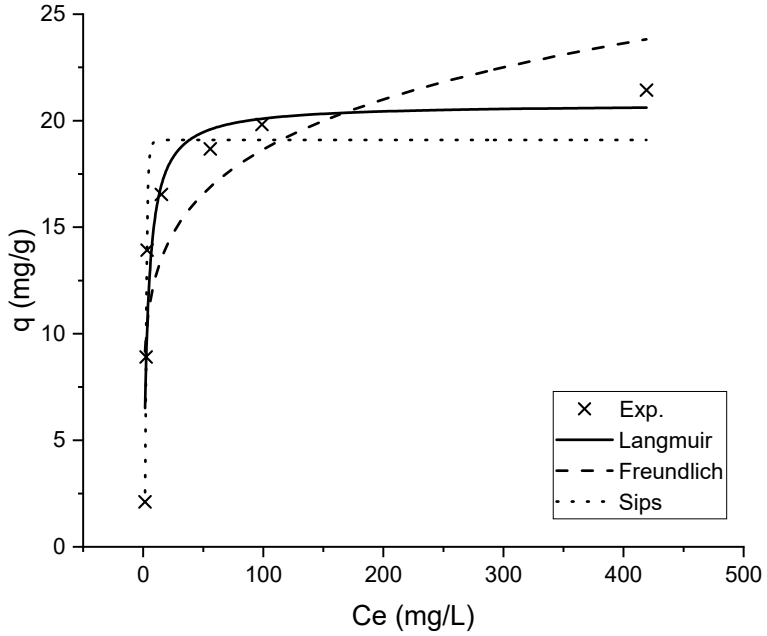


**Figure 5.** Langmuir, Freundlich, and Sips models applied to the experimental results.

### *3.6. Kinetic Studies*

Zn adsorption towards biomass-based carbon at room temperature is quite fast, as can be seen in Figure 6. Almost 80% removal can be achieved within the first 60 min. The adsorption equilibrium was attained at 240 min, and it remained constant thereafter. Maximum Zn removal and adsorption capacity were 95% and 14.4 mg/g, respectively. The fast removal of impurities is typical for carbonaceous adsorbents [34,44].

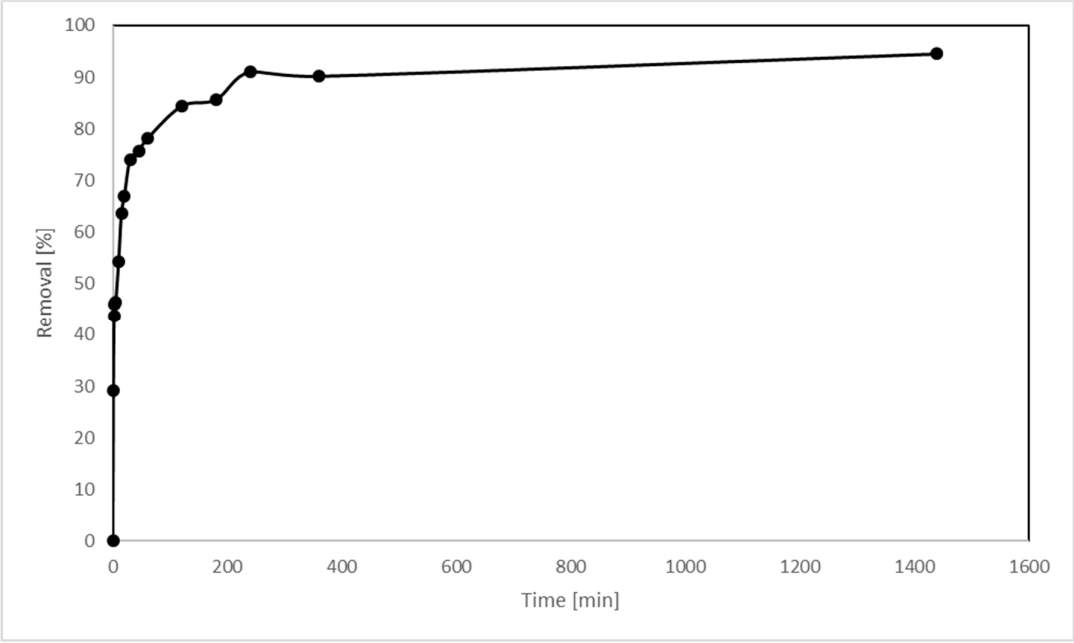


**Figure 6.** Zinc (Zn) removal [%] as a function of time (minutes). Experiments were done duplicated and the range of results were at maximum 3 percentage points.

Pseudo first-order, pseudo second-order, and Elovich kinetic models were applied to the experimental data. The obtained kinetic parameters are listed in Table 4, and fits are shown in Figure 7. The best fitting model was the Elovich model, with a correlation coefficient of 0.97 and an RMSE of 0.68. However, the correlation of the pseudo second-order model was also rarely good as it typically is for carbonaceous adsorbents [34,44]. The $R^2$ value was 0.94, and the calculated equilibrium removal (13.01 mg/g) was quite similar to the experimental one (14.36 mg/g). It can be seen in Figure 7 that the sorption process of the Zn removal did not take place immediately; rather, equilibrium was reached after a few hundred minutes. This is typical of processes following the Elovich model.

**Table 4.** Kinetic parameters of pseudo-first-order, pseudo-second-order, and Elovich models.

| Model | Parameter | Value |
|---|---|---|
| **Experiments** | $q_{e(exp)}$[mg/g] | 14.36 |
| | $q_{e(cal)}$ [mg/g] | 12.15 |
| **Pseudo-1-order** | $k_1$ [$min^{-1}$] | 0.22 |
| | $R^2$ | 0.83 |
| | RMSE | 1.66 |
| **Pseudo-2-order** | $q_{e(cal)}$ [mg/g] | 13.01 |
| | $k_2$ [g/ mg min] | 0.023 |
| | $R^2$ | 0.94 |
| | RMSE | 1.04 |
| **Elovich** | $\beta$ [g/mg] | 0.69 |
| | $\upsilon_0$ [mg/ g min] | 60.28 |
| | $R^2$ | 0.97 |
| | RMSE | 0.68 |

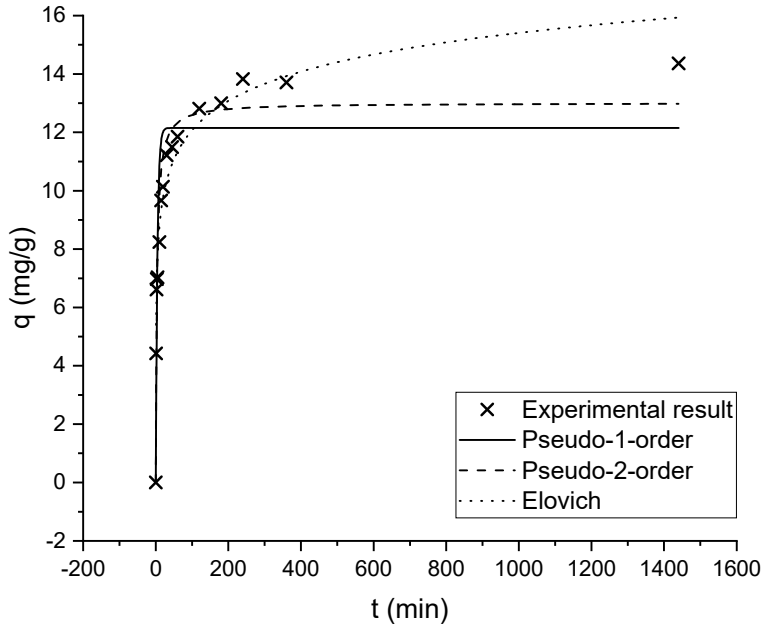


**Figure 7.** Pseudo-first-order, pseudo-second-order, and Elovich models applied to the experimental results.

### *3.7. Weber–Morris Model*

The Weber–Morris intraparticle diffusion model was applied to the kinetic data of biomass-based carbon against the $Zn^{2+}$. If a plot of $q_t$ versus $t^{1/2}$ presents a straight line from the origin, the adsorption mechanism only follows the intraparticle diffusion process. As can be seen in Figure 8, the data of $Zn^{2+}$ sorption on biomass-based carbon shows four plots that do not pass through the origin. The first stages can be attributed to the instantaneous or external surface adsorption. The majority of $Zn^{2+}$ ions are diffused through the solution to the external surface of the adsorbent in which the instantaneous sorption takes place. In the second stage, the adsorption capacity increases only slightly. This stage can be attributed to the slow diffusion of $Zn^{2+}$ ions from the surface sites into inner pores. In the third stage, the adsorption rate stays almost constant due to the low $Zn^{2+}$ ion concentration left in the solution [45,46].

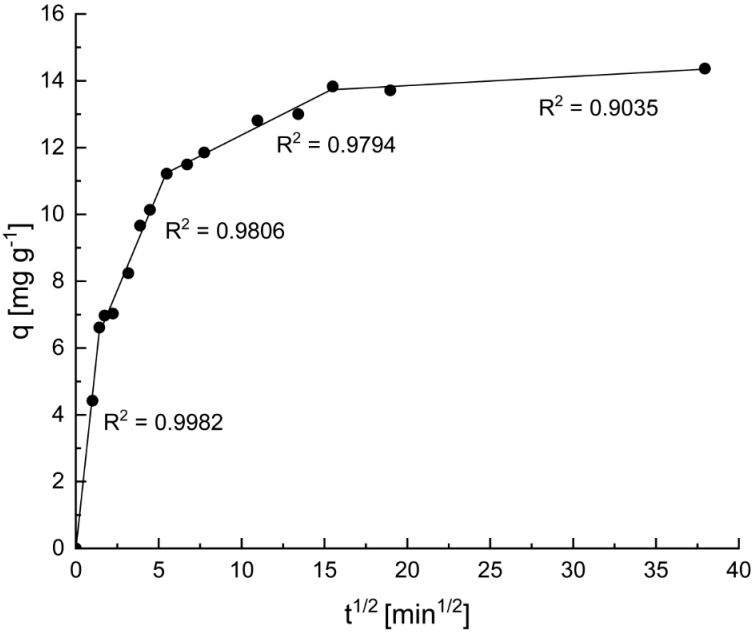


**Figure 8.** Weber–Morris intraparticle diffusion model.

### *3.8. Thermodynamic Effect of Temperature*

The effect of temperature on adsorption was studied by performing the experiments at three different temperatures (10 °C, 22 °C, and 40 °C) to study how the adsorption system works in colder environments or for higher temperature process waters. The removal percentages at 10 °C, 22 °C, and 44 °C were 88%, 91%, and 92%, respectively. Therefore, temperature has no meaningful effect on Zn removal, and the produced material can be used effectively in a wide temperature range.

Experiments were performed at three different temperatures, 10 °C, 20 °C, and 40 °C, and the results were used to calculate the parameters of the Van't Hoff plot (paragraph 2.6, Equation (8)). $\Delta H^0$ was calculated from the slope of the plot, and $\Delta S^0$ was calculated from the intercept of the plot. In addition, Gibbs free energies $\Delta G^0$ were calculated utilizing Equation (10). All the values are shown in Table 5, and the plot is presented in Figure 9.

The obtained $\Delta G^0$ values are negative, indicating that the adsorption process is spontaneous. The positive value of $\Delta S^0$ indicates that entropy is increasing in the process, and the positive $\Delta H^0$ value, which is smaller than 40 kJ/mol, refers to endothermic physisorption [47,48].

**Table 5.** Thermodynamic parameters of Zinc (Zn) sorption on the biomass-based activated carbon.

| Temperature (°C) | ΔG° (kJ/mol) | ΔS° (J/mol K) | ΔH° (kJ/mol) |
|---|---|---|---|
| **10** | −17.06 | | |
| **23** | −18.50 | 110.15 | 14.00 |
| **40** | −20.42 | | |

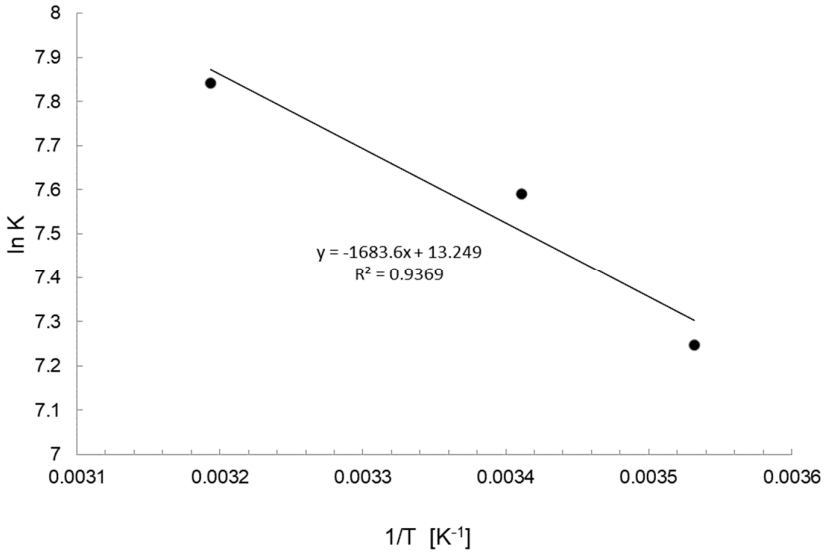


**Figure 9.** Van't Hoff plot of zinc (Zn) sorption on the biomass based activated carbon.

*3.9. Desorption Experiments*

After adsorption, the used adsorbents can be disposed of or regenerated; in both cases, there will be secondary pollution. Metal-loaded, used adsorbents are toxic for humans and the environment. In regeneration, metals are recovered in the solution form, and secondary pollution is caused by the regeneration solution [1]. Therefore, the regeneration solution used plays an important role, and the use of non-hazardous regeneration solutions is preferred. The regeneration solutions typically used are HCl [49,50], $H_2SO_4$ [36], 1 M KCl [35], 0.01 M $NaNO_3$ [51], and NaCl [52]. The regenerability of adsorbents is vital to enable cost-efficiency. In this study, Zn desorption was done using 0.1 M HCl; the results of the desorption experiments are presented in Figure 10. The desorption occurred immediately after the used adsorbent came into contact with the desorption solution. The desorption percentage was 80%, which was not related to the time. Therefore, it is possible to regenerate biomass-based carbon quickly using non-hazardous chemicals.

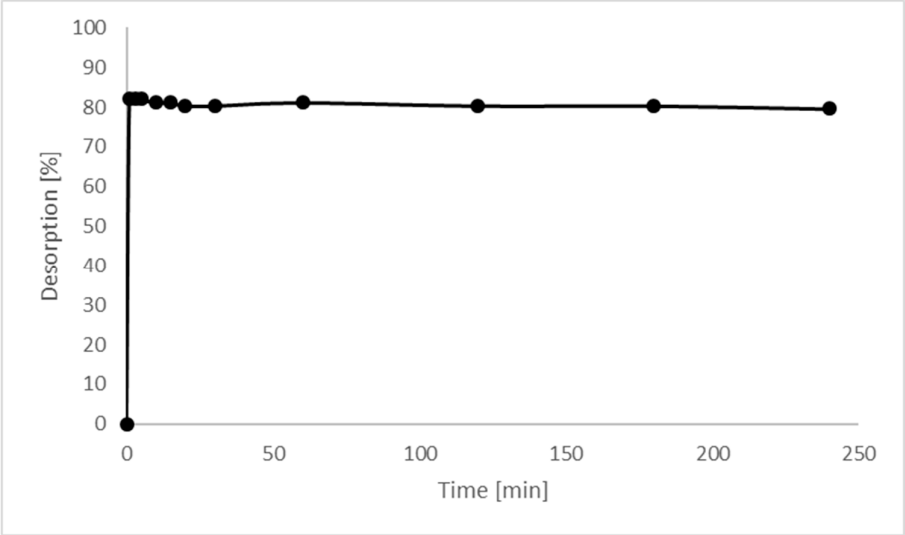


**Figure 10.** Desorption [%] as a function of time [min].

## 4. Conclusions

The adsorption of Zn(II) ions on biomass-based activated carbon was studied as a function of pH, solution metal–ion concentration, adsorbent dosage, time, and temperature. The amount (expressed as a %) of adsorbed Zn was the highest at pH 4. The removal percentage increased to 75 mg/L as a function of the initial Zn concentration, but the studied carbon adsorbent worked quite well at the 150 mg/L concentration level. The optimum adsorbent dosage was 3 g/L or 5 g/L. Zn adsorption onto the biomass-based activated carbon was not temperature-dependent. The adsorption isotherm followed the Sips isotherm and the Elovich kinetic model. Thermodynamic calculations showed that the adsorption process is spontaneous (negative $\Delta G^0$), that entropy increases during adsorption (positive $\Delta S^0$), and that the adsorption process consists of endothermic physisorption ($\Delta H^0$ smaller than 40 kJ/mol). The adsorption capacity obtained for biomass-based activated carbon was compared favorably to other adsorbents used in Zn removal presented in literature. As a conclusion, the suitable adsorbent for Zn removal from waste biomass was developed by using non-hazardous materials. The adsorbent can be used with wide temperature range and with quite high concentration range.

**Author Contributions:** S.T., H.R. (Henrik Romar), D.B., and R.K. were responsible for the conceptualization of the paper; S.T., H.R. (Henrik Romar), D.B., and R.K. were responsible for the methodology; H.R. (Hanna Runtti) and T.K. were responsible for the software used; R.K. was responsible for the investigation; all authors were responsible for the resources; S.T., R.K., T.K., and H.R. (Hanna Runtti) were responsible for the data curation; S.T. was responsible for preparing and writing the original draft; all authors were responsible for writing, reviewing, and editing; R.K., T.K., and H.R. (Hanna Runtti) were responsible for visualization; H.R. (Hanna Runtti) was responsible for supervision; U.L. was responsible for project administration; and U.L. was responsible for funding acquisition.

**Funding:** This work was done under the auspices of the Waterpro (ERDF project number: A74635, funded by the Central Ostrobothnia Regional Council). The author thanks Maa-ja Vesitekniikan Tuki Ry for the financial support.

**Conflicts of Interest:** The authors declare no conflict of interest. The funders had no role in the design of the study; in the collection, analyses, or interpretation of data; in the writing of the manuscript, or in the decision to publish the results.

## References

1. Tzou, Y.; Wang, S.; Hsu, L.; Chang, R.; Lin, C. Deintercalation of Li/Al LDH and its application to recover adsorbed chromate from used adsorbent. *Appl. Clay Sci.* **2007**, *37*, 107–114. doi:10.1016/j.clay.2006.10.007.

2. O'Connell, D.W.; Birkinshaw, C.; O'Dwyer, T.F. Heavy metal adsorbents prepared from the modification of cellulose: A review. *Bioresour. Technol.* **2008**, *99*, 6709–6724. doi:10.1016/j.biortech.2008.01.036.
3. Nicholson, F.A.; Smith, S.R.; Alloway, B.J.; Carlton-Smith, C.; Chambers, B.J. An inventory of heavy metals inputs to agricultural soils in England and Wales. *Sci. Total Environ.* **2003**, *311*, 205–219. doi:10.1016/S0048-9697(03)00139-6.
4. Rule, K.L.; Comber, S.D.W.; Ross, D.; Thornton, A.; Makropoulos, C.K.; Rautiu, R. Diffuse sources of heavy metals entering an urban wastewater catchment. *Chemosphere* **2006**, *63*, 64–72. doi:10.1016/j.chemosphere.2005.07.052.
5. Fernández, Y.; Marañón, E.; Castrillón, L.; Vázquez, I. Removal of Cd and Zn from inorganic industrial waste leachate by ion exchange. *J. Hazard. Mater.* **2005**, *126*, 169–175. doi:10.1016/j.jhazmat.2005.06.016.
6. Castelblanque, J.; Salimbeni, F. NF and RO membranes for the recovery and reuse of water and concentrated metallic salts from waste water produced in the electroplating process. *Desalination* **2004**, *167*, 65–73. doi:10.1016/j.desal.2004.06.114.
7. Mansoorian, H.J.; Mahvi, A.H.; Jafari, A.J. Removal of lead and zinc from battery industry wastewater using electrocoagulation process: Influence of direct and alternating current by using iron and stainless steel rod electrodes. *Sep. Purif. Technol.* **2014**, *135*, 165–175. doi:10.1016/j.seppur.2014.08.012.
8. Kurniawan, T.A.; Chan, G.Y.S.; Lo, W.; Babel, S. Physico-chemical treatment techniques for wastewater laden with heavy metals. *Chem. Eng. J.* **2006**, *118*, 83–98. doi:10.1016/j.cej.2006.01.015.
9. Laura, M. Plum, Lothar Rink and Hajo Haase the essential toxin: Impact of zinc on human health. *Int. J. Environ. Res. Public Health* **2010**, *7*, 1342–1365. doi:10.3390/ijerph7041342.
10. Fu, F.; Wang, Q. Removal of heavy metal ions from wastewaters: A review. *J. Environ. Manag.* **2011**, *92*, 407–418. doi:10.1016/j.jenvman.2010.11.011.
11. Demirbas, A. Heavy metal adsorption onto agro-based waste materials: A review. *J. Hazard. Mater.* **2008**, *157*, 220–229. doi:10.1016/j.jhazmat.2008.01.024.
12. Runtti, H.; Tuomikoski, S.; Kangas, T.; Lassi, U.; Kuokkanen, T.; Rämö, J. Chemically activated carbon residue from biomass gasification as a sorbent for iron(II), copper(II) and nickel(II) ions. *J. Water Process Eng.* **2014**, *4*, 12–24. doi:10.1016/j.jwpe.2014.08.009.
13. Ahmadpour, A.; Do, D.D. The preparation of activated carbon from macadamia nutshell by chemical activation. *Carbon* **1997**, *35*, 1723–1732. doi:10.1016/S0008-6223(97)00127-9.
14. Lussier, M.G.; Shull, J.C.; Miller, D.J. Activated carbon from cherry stones. *Carbon* **1994**, *32*, 1493–1498. doi:10.1016/0008-6223(94)90144-9.
15. Ricordel, S.; Taha, S.; Cisse, I.; Dorange, G. Heavy metals removal by adsorption onto peanut husks carbon: Characterization, kinetic study and modeling. *Sep. Purif. Technol.* **2001**, *24*, 389–401. doi:10.1016/S1383-5866(01)00139-3.
16. Kumar, J.; Balomajumder, C.; Mondal, P. Application of agro-based biomasses for zinc removal from wastewater—A review. *Clean Soil Air Water* **2011**, *39*, 641–652. doi:10.1002/clen.201000100.
17. Mishra, V.; Majumder, C.B.; Agarwal, V.K. Sorption of Zn(II) ion onto the surface of activated carbon derived from eucalyptus bark saw dust from industrial wastewater: Isotherm, kinetics, mechanistic modeling, and thermodynamics. *Desalin. Water Treat.* **2012**, *46*, 332–351. doi:10.1080/19443994.2012.677556.
18. Mohan, D.; Singh, K.P. Single- and multi-component adsorption of cadmium and zinc using activated carbon derived from bagasse—An agricultural waste. *Water Res.* **2002**, *36*, 2304–2318. doi:10.1016/S0043-1354(01)00447-X.
19. Bergna, D.; Varila, T.; Romar, H.; Lassi, U. Comparison of the properties of activated carbons produced in one-stage and two-stage processes. *C* **2018**, *4*, 41. doi:10.3390/c4030041.
20. Azargohar, R.; Dalai, A.K. Production of activated carbon from Luscar char: Experimental and modeling studies. *Microporous Mesoporous Mater.* **2005**, *85*, 219–225. doi:10.1016/j.micromeso.2005.06.018.
21. Marsh, H.; Rodríguez-Reinoso, F. (Eds.) CHAPTER 5—Activation processes (thermal or physical). In *Activated Carbon*; Elsevier Science Ltd.: Oxford, UK, 2006; pp. 243–321. doi:10.1016/B978-008044463-5/50019-4.
22. Bansal, R.C.; Goyal, M. *Activated Carbon Adsorption*; CRC Press: Boca Raton, FL, USA, 2005; doi:10.1201/9781420028812.
23. Williams, P.T.; Reed, A.R. Development of activated carbon pore structure via physical and chemical activation of biomass fibre waste. *Biomass Bioenergy* **2006**, *30*, 144–152. doi:10.1016/j.biombioe.2005.11.006.

24. Brunauer, S.; Emmett, P.H.; Teller, E. Adsorption of gases in multimolecular layers. *J. Am. Chem. Soc.* **1938**, *60*, 309–319. doi:10.1021/ja01269a023.
25. Barrett, E.P.; Joyner, L.G.; Halenda, P.P. The determination of pore volume and area distributions in porous substances. I. computations from nitrogen isotherms. *J. Am. Chem. Soc.* **1951**, *73*, 373–380. doi:10.1021/ja01145a126.
26. Langmuir, I. The adsorption of gases on plane surfaces of glass, mica and platinum. *J. Am. Chem. Soc.* **1918**, *40*, 1361–1403. doi:10.1021/ja02242a004.
27. Freundlich, H. Over the adsorption in solution. *J. Phys. Chem.* **1906**, *57*, 385–471.
28. Sips, R. On the structure of a catalyst surface. *J. Chem. Phys.* **1948**, *16*, 490–495. doi:10.1063/1.1746922.
29. Lagergren, S. About the theory of so-called adsorption of soluble substances. *K. Sven. Vetensk. Handl.* **1898**, *24*, 1–39.
30. Ho, Y.S.; McKay, G. Pseudo-second order model for sorption processes. *Process Biochem.* **1999**, *34*, 451–465. doi:10.1016/S0032-9592(98)00112-5.
31. Zeldowitsch, J. Über den mechanismus der katalytischen oxydation von CO an MnO2 [About the mechanism of catalytic oxidation of CO over MnO2]. *Acta Physicochim URSS* **1934**, *1*, 364–449.
32. Weber, W.J.; Morris, J.C. Kinetics of adsorption on carbon from solutions. *J. Sanit. Eng. Div. Am. Soc. Civil Eng.* **1963**, *89*, 31–60.
33. Riikka, L.; Davide, B.; Henrik, R.; Tero, T.; Tao, H.; Ulla, L. Physico-chemical properties and use of waste biomass-derived activated carbons. *Chem. Eng. Trans.* **2017**, *57*, 43–48.
34. Kilpimaa, S.; Runtti, H.; Kangas, T.; Lassi, U.; Kuokkanen, T. Physical activation of carbon residue from biomass gasification: Novel sorbent for the removal of phosphates and nitrates from aqueous solution. *J. Ind. Eng. Chem.* **2015**, *21*, 1354–1364. doi:10.1016/j.jiec.2014.06.006.
35. Katsou, E.; Malamis, S.; Tzanoudaki, M.; Haralambous, K.J.; Loizidou, M. Regeneration of natural zeolite polluted by lead and zinc in wastewater treatment systems. *J. Hazard. Mater.* **2011**, *189*, 773–786. doi:10.1016/j.jhazmat.2010.12.061.
36. Motsi, T.; Rowson, N.A.; Simmons, M.J.H. Adsorption of heavy metals from acid mine drainage by natural zeolite. *Int. J. Miner. Process.* **2009**, *92*, 42–48. doi:10.1016/j.minpro.2009.02.005.
37. Covelo, E.F.; Vega, F.A.; Andrade, M.L. Competitive sorption and desorption of heavy metals by individual soil components. *J. Hazard. Mater.* **2007**, *140*, 308–315. doi:10.1016/j.jhazmat.2006.09.018.
38. Marshall, W.E.; Johns, M.M. Agricultural by-products as metal adsorbents: Sorption properties and resistance to mechanical abrasion. *J. Chem. Technol. Biotechnol.* **1996**, *66*, 192–198. doi:10.1002/(SICI)1097-4660(199606)66:2.
39. Gharaibeh, S.H.; Abu-el-sha'r, W.Y.; Al-Kofahi, M.M. Removal of selected heavy metals from aqueous solutions using processed solid residue of olive mill products. *Water Res.* **1998**, *32*, 498–502. doi:10.1016/S0043-1354(97)00221-2.
40. Ferro-García, M.A.; Rivera-Utrilla, J.; Rodríguez-Gordillo, J.; Bautista-Toledo, I. Adsorption of zinc, cadmium, and copper on activated carbons obtained from agricultural by-products. *Carbon* **1988**, *26*, 363–373. doi:10.1016/0008-6223(88)90228-X.
41. Budinova, T.K.; Petrov, N.V.; Minkova, V.N.; Gergova, K.M. Removal of metal ions from aqueous solution by activated carbons obtained from different raw materials. *J. Chem. Technol. Biotechnol.* **1994**, *60*, 177–182. doi:10.1002/jctb.280600210.
42. Allen, S.J.; Brown, P.A. Isotherm analyses for single component and multi-component metal sorption onto lignite. *J. Chem. Technol. Biotechnol.* **1995**, *62*, 17–24. doi:10.1002/jctb.280620103.
43. McKay, G.; Porter, J.F. Equilibrium parameters for the sorption of copper, cadmium and zinc ions onto peat. *J. Chem. Technol. Biotechnol.* **1997**, *69*, 309–320. doi:10.1002/(SICI)1097-4660(199707)69:3.
44. Hanna, R.; Sari, T.; Teija, K.; Toivo, K.; Jaakko, R.; Ulla, L. Sulphate removal from water by carbon residue from biomass gasification: Effect of chemical modification methods on sulphate removal efficiency. *BioResources* **2016**, *11*, 3136–3152.
45. Caliskan, N.; Kul, A.R.; Alkan, S.; Sogut, E.G.; Alacabey, İ. Adsorption of Zinc(II) on diatomite and manganese-oxide-modified diatomite: A kinetic and equilibrium study. *J. Hazard. Mater.* **2011**, *193*, 27–36. doi:10.1016/j.jhazmat.2011.06.058.
46. Arias, F.; Sen, T.K. Removal of zinc metal ion (Zn2+) from its aqueous solution by kaolin clay mineral: A kinetic and equilibrium study. *Colloids Surf. A Physicochem. Eng. Asp.* **2009**, *348*, 100–108. doi:10.1016/j.colsurfa.2009.06.036.

47. Katal, R.; Baei, M.S.; Rahmati, H.T.; Esfandian, H. Kinetic, isotherm and thermodynamic study of nitrate adsorption from aqueous solution using modified rice husk. *J. Ind. Eng. Chem.* **2012**, *18*, 295–302. doi:10.1016/j.jiec.2011.11.035.
48. Bhatnagar, A.; Kumar, E.; Sillanpää, M. Nitrate removal from water by nano-alumina: Characterization and sorption studies. *Chem. Eng. J.* **2010**, *163*, 317–323. doi:10.1016/j.cej.2010.08.008.
49. Iqbal, M.; Saeed, A.; Akhtar, N. Petiolar felt-sheath of palm: A new biosorbent for the removal of heavy metals from contaminated water. *Bioresour. Technol.* **2002**, *81*, 151–153.
50. Saeed, A.; Akhter, M.W.; Iqbal, M. Removal and recovery of heavy metals from aqueous solution using papaya wood as a new biosorbent. *Sep. Purif. Technol.* **2005**, *45*, 25–31. doi:10.1016/j.seppur.2005.02.004.
51. Hu, J.; Shipley, H.J. Evaluation of desorption of Pb (II), Cu (II) and Zn (II) from titanium dioxide nanoparticles. *Sci. Total Environ.* **2012**, *431*, 209–220. doi:10.1016/j.scitotenv.2012.05.039.
52. Xu, W.; Li, L.Y.; Grace, J.R. Regeneration of natural Bear River clinoptilolite sorbents used to remove Zn from acid mine drainage in a slurry bubble column. *Appl. Clay Sci.* **2012**, *55*, 83–87. doi:10.1016/j.clay.2011.10.009.